PHYSICAL REVIEW D **88,** 034008 (2013)

Towards two-body strong decay behavior of higher ρ and ρ_3 mesons

Li-Ping He,* Xiao Wang,† and Xiang Liu‡

School of Physical Science and Technology, Lanzhou University, Lanzhou 730000, China

Research Center for Hadron and CSR Physics, Lanzhou University and Institute of Modern Physics of CAS, Lanzhou 730000, China

(Received 25 June 2013; published 6 August 2013)

In this work, we systematically study the two-body strong decay of the ρ/ρ_3 states, which are observed and grouped into the ρ/ρ_3 meson family. By performing the phenomenological analysis, the underlying properties of these states are obtained and tested. What is more important is that abundant information of their two-body strong decays is predicted, which will be helpful to further and experimentally study these states.

DOI: 10.1103/PhysRevD.88.034008 PACS numbers: 14.40.Be, 12.38.Lg, 13.25.Jx

I. INTRODUCTION

There is abundant information on ρ/ρ_3 states collected by the Particle Data Group (PDG) [1], which provides that their spin-parity J^P could be $1^-/3^-$ and all of them are isovector. In Table I, we briefly review the resonance parameters of the observed ρ/ρ_3 states. As the total angular momentum J increases, the number of these states decreases.

The experimental status of these states stimulates our interest in revealing their underlying structures, since at present the properties of ρ/ρ_3 are still in chaos. First of all, we need to examine whether these ρ/ρ_3 can be categorized into the conventional meson family. Besides the study of mass spectrum, their Okubo-Zweig-Iizuka (OZI)—allowed two-body strong decay behaviors can reflect important information on their structures. Thus, in this work we make more effort to systematically calculate the OZI-allowed strong decays of ρ/ρ_3, where the quark pair creation (QPC) model will be applied to the calculation. Before carrying out the calculation, we need to determine the corresponding radial, orbital, and spin quantum numbers to these ρ/ρ_3, where we can refer to the analysis of mass spectrum, which will be summarized in the following section. By comparing our results with the experimental data, the meson assignment to these observed ρ/ρ_3 should be examined. Additionally, our obtained OZI-allowed two-body strong decay behaviors will provide valuable information for further experimental study on ρ/ρ_3.

As mentioned above, this phenomenological study on ρ/ρ_3 can be applied to distinguish their possible meson assignments. In addition, by this work, we can learn what state is not suitable to be interpreted as conventional meson state. Thus, our study may provide important insights on whether these studies are relevant to exotic hadron configuration or new novel mechanisms.

*help08@lzu.edu.cn
†xiaowang2011@lzu.edu.cn
‡Corresponding author.
xiangliu@lzu.edu.cn

This paper is organized as follows. After the Introduction, we briefly review the present research status of these ρ/ρ_3. In Sec. III, we discuss the possible meson assignment to these states, using the mass spectrum analysis and introduce the QPC model. The allowed decay channels are also selected. In Sec. IV, we perform the phenomenological analysis of ρ/ρ_3. The last section is devoted to a short summary.

II. REVIEW OF RESEARCH STATUS

As shown in Table I, there are many ρ/ρ_3 states observed by experiments. Among these states, $\rho(770)$ [8] is established to be the ground state with $n^{2S+1}L_J = 1^3S_1$ with very broad full width. Thus, we will not include $\rho(770)$ when briefly reviewing the research status of the ρ/ρ_3 states. In the following, we introduce the experimental and theoretical status of ρ/ρ_3.

TABLE I. The experimental information of the observed ρ/ρ_3 states. Here, the masses and widths (in units of MeV) are average values taken from PDG [1]. The states marked by the superscript ♭, are as the states omitted form the summary table of PDG, while the states marked by the superscript ♮ are as further states listed in PDG.

State	Mass	Width
	$J^P = 1^-$	
$\rho(770)$	775.49 ± 0.34	146.2 ± 0.7
$\rho(1450)$	1465 ± 25	400 ± 60
$\rho(1570)^\flat$	$1570 \pm 36 \pm 62$	$144 \pm 75 \pm 43$
$\rho(1700)$	1720 ± 20	250 ± 100
$\rho(1900)^\flat$ [2]	$1909 \pm 17 \pm 25$	$48 \pm 17 \pm 2$
$\rho(2150)^\flat$	2149 ± 17	359 ± 40
$\rho(2000)^\natural$ [3–6]	2000 ± 30	260 ± 45
$\rho(2270)^\natural$ [3–6]	2265 ± 40	325 ± 80
	$J^P = 3^-$	
$\rho_3(1690)$	1688.8 ± 2.1	161 ± 10
$\rho_3(1990)^\flat$ [3]	1982 ± 14	188 ± 24
$\rho_3(2250)^\flat$ [7]	~ 2232	~ 220

$\rho(1600)$ was omitted in the 1988 edition of PDG [9] and replaced by $\rho(1450)$ and $\rho(1700)$, which is due to many theoretical and experimental studies [10–27].

In the past decades, many efforts have been made to explain the structure of $\rho(1450)$. However, its property is still unclear at present. Although the study of the mass spectrum supports $\rho(1450)$ as a 2^3S_1 state [28], the decay behavior is hard to understand. The calculation in Ref. [29] shows that the $\pi\pi$ and $\omega\pi$ channels are dominant in the $\rho(1450)$ decays. Using the nonlocal Nambu-Jona-Lasinio model, the calculated partial widths of $\rho(1450) \to \pi\pi$ and $\rho(1450) \to \pi\omega$ are also comparable with the experimental values [30,31]. On the other hand, the theoretical decay widths of $\rho(1450) \to a_1(1260)\pi$ and $h_1(1170)\pi$ become small [29]. However, the experimental result indicates that $\rho(1450)$ mainly decays into 4π [1,17,23,32]. To alleviate the discrepancy between the experimental and theoretical results of the 4π channel, $\rho(1450)$ as a mixture of 2^3S_1 ρ state and hybrid was introduced in Ref. [29] since Close *et al.* indicated that the vector hybrid with mass about 1.5 GeV can strongly couple with $a_1(1260)\pi$ [33]. Other theoretical studies [33–36] also support this mixture.

Besides these two explanations for $\rho(1450)$ as mentioned above, explanation of $\rho(1450)$ as a 1^3D_1 state was proposed in Refs. [37,38] using the chiral symmetry method. If considering the mass spectrum analysis on the ρ meson family, we notice that the mass of the 1^3D_1 ρ meson should be 1600–1700 MeV [39]. This mass discrepancy cannot be ignored when explaining $\rho(1450)$ as a 1^3D_1 ρ meson.

$\rho(1700)$ is a good candidate of the 1^3D_1 ρ meson. Both the analysis of the branching ratio of $\rho(1700) \to 2\pi, 4\pi$ [32] and the study of $e^+e^- \to \omega\pi^0$ via the nonrelativistic $^3P_0$ quark model [40] show that $\rho(1700)$ is a 1^3D_1 state.

There are many experiments relevant to $\rho(1900)$. The DM2 Collaboration once reported a dip around 1.9 GeV by analyzing the $e^+e^- \to 6\pi$ process [21]. Later, the FENICE Collaboration observed a dip around 1.9 GeV in the R value measurement, which can be produced by the interference of a resonance with one of these broad vector mesons [41]. In 2001, the E687 Collaboration at Fermilab found a narrow dip structure at 1.9 GeV through the $3\pi^+3\pi^-$ diffractive photoproduction [42]. If this dip is due to a destructive interference of a resonance with a continuum background, the resonance parameters can be extracted as $m = (1.911 \pm 0.004 \pm 0.001)$ GeV and $\Gamma = (29 \pm 11 \pm 4)$ MeV. By refitting their data, the E687 Collaboration indicated that the interference effect of a narrow resonance with known vector mesons [such as a broad $\rho(1700)$] can result in a dip [43]. In both of $e^+e^- \to 3\pi^+3\pi^-$ and $e^+e^- \to 2\pi^+2\pi^-2\pi^0$ processes, the *BABAR* Collaboration announced the observation of a structure around 1.9 GeV [44], which was confirmed by *BABAR* in the $e^+e^- \to \phi\pi^0$ process [2]. The CMD3 Collaboration observed a peak near the $p\bar{p}$ threshold, which can be identified as $\rho(1900)$ [45]. In Ref. [39], Bugg indicated that this CMD3's observation can be explained to be a $^3S_1$ state captured by the very strong $p\bar{p}$ S-wave or to be a nonresonant cusp effect.

Analyzing the data of the 6π mass spectrum from the e^+e^- annihilation [46] and the diffractive photoproduction [47], Clegg and Donnachie indicated the existence of $\rho(2150)$ [48]. Later, Biagini *et al.* [49] suggested that there exists the third radial excitation of $\rho(770)$ by phenomenologically fitting the pion form factor [50], and gave the corresponding resonant parameters $m \simeq 2150$ MeV and $\Gamma \simeq 320$ MeV, which is consistent with the result in Ref. [48]. In addition, the GAMS Collaboration also confirmed the observation of $\rho(2150)$ in $\pi^-p \to \omega\pi^0 n$ [51,52]. In Refs. [3,4,6,53], the Crystal Barrel data was analyzed, where a 1^{--} resonance with the mass 2.15 GeV can be as the evidence of $\rho(2150)$. In 2007, *BABAR* observed $\rho(2150)$ in the new process $e^+e^- \to \eta'(958)\pi^+\pi^-$ and $f_1(1285)\pi^+\pi^-$ [54].

Godfrey and Isgur have predicted a 2^3D_1 state with mass 2.15 GeV [28], which can correspond to $\rho(2150)$. However, there exists another explanation to $\rho(2150)$; i.e., Anisovich *et al.* suggested $\rho(2150)$ to be a 4^3S_1 state [55], which was confirmed in Refs. [39,56,57].

In Table I there are two more states of 1^{--} listed in PDG [1], which are $\rho(2000)$ and $\rho(2270)$. In the $p\bar{p} \to \pi\pi$ reaction, a resonance around 1988 MeV was found [7]. Later, Anisovich *et al.* obtained a $J^{PC} = 1^{--}$ state at 2000 MeV in the same reaction [4], which also appears in the $p\bar{p} \to \omega\eta\pi^0$ and $\omega\pi$ processes [3,5,6]. $\rho(2000)$ was suggested as the radial excitation of $\rho(1700)$ [3]. In Ref. [58], Bugg concluded that $\rho(2000)$ can be a mixed state with a significant $^3D_1$ component.

In the reaction $\gamma p \to \omega\pi^+\pi^-\pi^0$, a resonance at 2280 ± 50 MeV was reported by the Omega Photon Collaboration [47]. The analysis of the Crystal Barrel data indicates that $\rho(2270)$ is important to fit the $\omega\eta\pi$ data, and can be ignored to describe the $\omega\pi$ data [3]. The Regge trajectory analysis shows that $\rho(2270)$ can be a 3^3D_1 state, i.e., the second radial excitation of $\rho(1700)$.

In PDG [1], there are three ρ_3 states. $\rho_3(1690)$ was first observed in Refs. [59,60], which was once regarded as a $\pi^+\pi^-$ resonance. At present, $\rho_3(1690)$ is established to be a $^3D_3$ state, which can decay into 2π, $K\bar{K}$, $K\bar{K}\pi$, 4π, $\omega\pi$, and $\eta\pi^+\pi^-$ as shown in PDG [1]. Additionally, two more new decay modes, $a_2(1320)\pi$ and $\rho\eta$, were reported in Ref. [61]. Besides the $^3D_3$ explanation for $\rho_3(1690)$, it could be interpreted as a three-rho meson molecular state in Ref. [62].

As a 3^{--} state, $\rho_3(1990)$ with $m \sim 2007$ MeV and $\Gamma \sim 287$ MeV was observed in the $\pi\pi$ invariant mass spectrum of $p\bar{p} \to \pi\pi$ [7], which was confirmed by analyzing the Crystal Barrel data [4,5,53], where a 3^{--} resonance exists in the $p\bar{p} \to \pi^+\pi^-$, $\omega\pi$ processes. The $\omega\eta\pi^0$ decay of $\rho_3(1990)$ was reported in Ref. [6]. In Ref. [3], a combined fit to the $\omega\pi$, $\omega\eta\pi^0$ and $\pi^-\pi^+$ data was performed, which gives the weighed mean of mass and width of $\rho_3(1990)$ as listed in Table I.

There are many experimental papers relevant to $\rho_3(2250)$ as shown in PDG [1]. $\rho_3(2250)$ was first observed by BNL through studying the S-channel $\bar{p}N$ cross section [63]. Later, $\rho_3(2250)$ was also found in the reactions $p\bar{p} \to \bar{p}p$ [64], $p\bar{p} \to \bar{N}N$ [65], $p\bar{p} \to K^+K^-$ [66], and $p\bar{p} \to \pi\pi$ [7,67–69]. In 2000, the VES Collaboration reported a 3^{--} resonance at 2290 MeV in the reaction $\pi^- p \to \eta\pi^+\pi^- n$ [61]. The analysis of the Crystal Barrel data for the $p\bar{p} \to \pi^-\pi^+$ [4], $p\bar{p} \to \omega\eta\pi^0$ [6] and $p\bar{p} \to \omega\pi$ [5] reactions also requires the existence of $\rho_3(2250)$.

A plot of the Regge trajectory for the mass spectrum of the 3^{--} states was presented in Refs. [3–5], where $\rho_3(1990)$ and $\rho_3(2250)$ are treated as the 2^3D_3 and 3^3D_3 states, respectively.

III. TWO-BODY STRONG DECAYS

Before carrying out the study of the two-body strong decay of these ρ/ρ_3 states shown in Table I, we need to illustrate the analysis of their Regge trajectory.

The analysis of the Regge trajectory is an effective approach to quantitatively study meson mass spectrum. In general, there exists an expression [55,70],

$$M^2 = M_0^2 + (n-1)\mu^2, \tag{1}$$

where M_0 is the mass of ground state and μ^2 denotes the trajectory slope and n is the radial quantum number of the corresponding meson with mass M. The relation expressed by Eq. (1) is roughly satisfied by ρ/ρ_3 states as shown in Fig. 1, which indicates

(1) $\rho(1450)$, $\rho(1900)$, and $\rho(2150)$ are the radial excitations of $\rho(770)$.
(2) $\rho(1700)$, $\rho(2000)$, and $\rho(2270)$ can be grouped into the n^3D_1 ρ meson family. Among these three states, $\rho(1700)$ is the ground state while $\rho(2000)$ and $\rho(2270)$ are the first and the second radial excitations of $\rho(1700)$.
(3) $\rho_3(1690)$, $\rho_3(1990)$, and $\rho_3(2250)$ can be as good candidates of the 1^3D_3, 2^3D_3, and 3^3D_3 states, respectively.

Figure 1 only gives a rough estimate of categorizing ρ/ρ_3 states into the meson families. A further study of their two-body strong decay behaviors can test whether the assignment shown in Fig. 1 is reasonable. Here, the QPC model is adopted to calculate the partial decay widths of these decays.

The QPC model was first proposed by Micu [71] and further developed by the Orsay group [72–76]. It is has been widely adopted to study the OZI-allowed strong decay of hadrons [77–99]. For depicting a quark-antiquark pair created from the vacuum, a transition operator $\mathcal{T}$ is introduced by

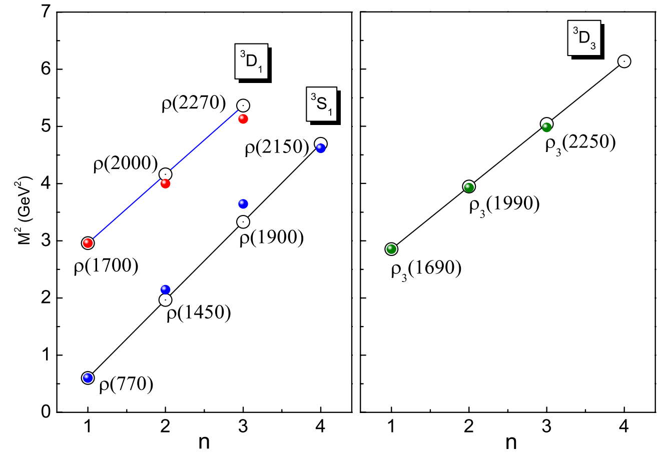

FIG. 1 (color online). The analysis of the Regge trajectories for the ρ/ρ_3 states. The trajectory slopes are 1.365 GeV^2, 1.203 GeV^2, and 1.094 GeV^2 for the $^3S_1$, $^3D_1$, and $^3D_3$ states, respectively. ⊙ denotes the theoretical values, while the red, blue, and green dots correspond to the experimental data listed in Table I.

$$\mathcal{T} = -3\gamma\sum_m \langle 1m; 1-m|00\rangle \times \int d^3\mathbf{p}_3 d^3\mathbf{p}_4 \delta^3(\mathbf{p}_3+\mathbf{p}_4)\mathcal{Y}_{1m}\left(\frac{\mathbf{p}_3-\mathbf{p}_4}{2}\right) \times \chi^{34}_{1,-m}\phi^{34}_0\omega^{34}_0 b^\dagger_{3i}(\mathbf{p}_3)d^\dagger_{4j}(\mathbf{p}_4). \tag{2}$$

Here, $\mathbf{p}_3/\mathbf{p}_4$ denotes the three-momentum of quark/antiquark created from the vacuum. Thus, the transition matrix element of the $A \to B + C$ process can be expressed as

$$\langle BC|\mathcal{T}|A\rangle = \delta^3(\mathbf{P}_B + \mathbf{P}_C)\mathcal{M}^{M_{J_A}M_{J_B}M_{J_C}}, \tag{3}$$

where $\mathbf{P}_B/\mathbf{P}_C$ is the three-momentum of the final state hadron B/C in the center-of-mass frame of the initial state A. In Eq. (3), $\mathcal{Y}_{\ell m}(\mathbf{p}) \equiv |\mathbf{p}|^\ell Y_{\ell m}(\theta_p, \phi_p)$ denotes the ℓth solid harmonic polynomial, $\chi^{34}_{1,-m}$ is a spin triplet state, and i and j are the $SU(3)$ color indices of the created quark pairs from the vacuum. $\phi^{34}_0 = (u\bar{u} + d\bar{d} + s\bar{s})/\sqrt{3}$ describes flavor singlet and $\omega^{34}_0 = \delta_{\alpha_3\alpha_4}/\sqrt{3}$ ($\alpha = 1, 2, 3$) corresponds to color singlet.

By the Jacob-Wick formula [100], the decay amplitude is expressed as

$$\mathcal{M}^{JL}(A \to BC) = \frac{\sqrt{2L+1}}{2J_A+1}\sum_{M_{J_B},M_{J_C}} \langle L0; JM_{J_A}|J_A M_{J_A}\rangle \times \langle J_B M_{J_B}; J_C M_{J_C}|JM_{J_A}\rangle \mathcal{M}^{M_{J_A}M_{J_B}M_{J_C}}.$$

Furthermore, the decay width reads as

$$\Gamma_{A\to BC} = \pi^2 \frac{|\mathbf{P}_B|}{m_A^2}\sum_{J,L}|\mathcal{M}^{JL}|^2, \tag{4}$$

where m_A is the mass of the initial state A. In the concrete calculation, the harmonic oscillator wave function,

$$\Psi_{n,\ell,m}(R,\mathbf{q}) = \mathcal{R}_{n,\ell}(R,\mathbf{q})\mathcal{Y}_{\ell m}(\mathbf{q}), \quad (5)$$

is applied to describe the meson wave function. In the QPC model, the two parameters R and γ are introduced. Here, R can be determined by reproducing the realistic root mean square radius, which is obtained by solving the Schrödinger equation with the potential in Ref. [88]. Although the R values can be obtained by the above approach in principle, these values are to be used for reference only. Thus, we illustrate the calculated partial decay widths of these ρ and ρ_3 states in terms of parameter R within a typical range of values. γ is a dimensionless constant for describing the strength of the quark pair creation. By systematically fitting the experimental data, $\gamma = 8.7$ is obtained for $u\bar{u}/d\bar{d}$ pair creation (see Table II in Ref. [99] for more details in extracting the γ value), while the strength of the $s\bar{s}$ pair creation satisfies $\gamma = 8.7/\sqrt{3}$ [75].

In Table II, the allowed two-body strong decay channels of ρ/ρ_3 are listed. Using the QPC model, we obtain the

TABLE II. The OZI-allowed two-body decay modes of the ρ/ρ_3 states. Here, ω, ρ, and η' denote $\omega(782)$, $\rho(770)$, and $\eta'(958)$, respectively. The allowed two-body decays are marked by ✓.

	$\pi\pi$	$\pi h_1(1170)$	$\pi\pi(1300)$	$\pi\omega(1420)$	$\pi\omega(1650)$	$\rho b_1(1235)$	$\rho f_1(1285)$	$\omega a_1(1260)$	$\eta\rho(1450)$	$\rho f_1(1420)$
$\rho(1450)$	✓	✓	✓							
$\rho(1700)$	✓	✓	✓	✓						
$\rho(1900)$	✓	✓	✓	✓	✓					
$\rho(2000)$	✓	✓	✓	✓	✓					
$\rho(2150)$	✓	✓	✓	✓	✓	✓	✓	✓	✓	
$\rho(2270)$	✓	✓	✓	✓	✓	✓	✓	✓	✓	✓
$\rho_3(1690)$	✓	✓	✓	✓						
$\rho_3(1990)$	✓	✓	✓	✓	✓					
$\rho_3(2250)$	✓	✓	✓	✓	✓	✓	✓	✓	✓	✓

	$\pi\omega$	$\pi a_1(1260)$	$\pi a_2(1320)$	$\pi a_0(1450)$	$\pi\omega_3(1670)$	$\rho f_2(1270)$	$\rho\eta(1295)$	$\omega\pi(1300)$	$\pi a_4(2040)$	$\rho\rho(1450)$
$\rho(1450)$	✓	✓	✓							
$\rho(1700)$	✓	✓	✓	✓						
$\rho(1900)$	✓	✓	✓	✓	✓					
$\rho(2000)$	✓	✓	✓	✓	✓					
$\rho(2150)$	✓	✓	✓	✓	✓	✓	✓	✓	✓	
$\rho(2270)$	✓	✓	✓	✓	✓	✓	✓	✓	✓	✓
$\rho_3(1690)$	✓	✓	✓	✓						
$\rho_3(1990)$	✓	✓	✓	✓	✓					
$\rho_3(2250)$	✓	✓	✓	✓	✓	✓	✓	✓	✓	✓

	$\eta\rho$	$\rho\rho$	$\rho\eta'$	$\eta b_1(1235)$	$\pi\pi_2(1670)$	$\pi\pi(1800)$	$\omega a_2(1320)$	$\eta\rho_3(1690)$	$\rho\eta(1475)$	$\omega a_0(1450)$
$\rho(1450)$	✓									
$\rho(1700)$	✓	✓								
$\rho(1900)$	✓	✓	✓	✓	✓					
$\rho(2000)$	✓	✓	✓	✓	✓	✓				
$\rho(2150)$	✓	✓	✓	✓	✓	✓	✓			
$\rho(2270)$	✓	✓	✓	✓	✓	✓	✓	✓	✓	✓
$\rho_3(1690)$	✓	✓								
$\rho_3(1990)$	✓	✓	✓	✓	✓	✓				
$\rho_3(2250)$	✓	✓	✓	✓	✓	✓	✓	✓	✓	

	KK	KK^*	K^*K^*	$KK_1(1270)$	$KK_1(1400)$	$KK^*(1410)$	$KK_2^*(1430)$	$KK^*(1680)$	$K^*K_1(1270)$	$\eta' b_1(1235)$
$\rho(1450)$	✓	✓								
$\rho(1700)$	✓	✓								
$\rho(1900)$	✓	✓	✓	✓	✓					
$\rho(2000)$	✓	✓	✓	✓	✓	✓	✓			
$\rho(2150)$	✓	✓	✓	✓	✓	✓	✓			
$\rho(2270)$	✓	✓	✓	✓	✓	✓	✓	✓	✓	✓
$\rho_3(1690)$	✓	✓								
$\rho_3(1990)$	✓	✓	✓	✓	✓	✓	✓			
$\rho_3(2250)$	✓	✓	✓	✓	✓	✓	✓	✓	✓	✓

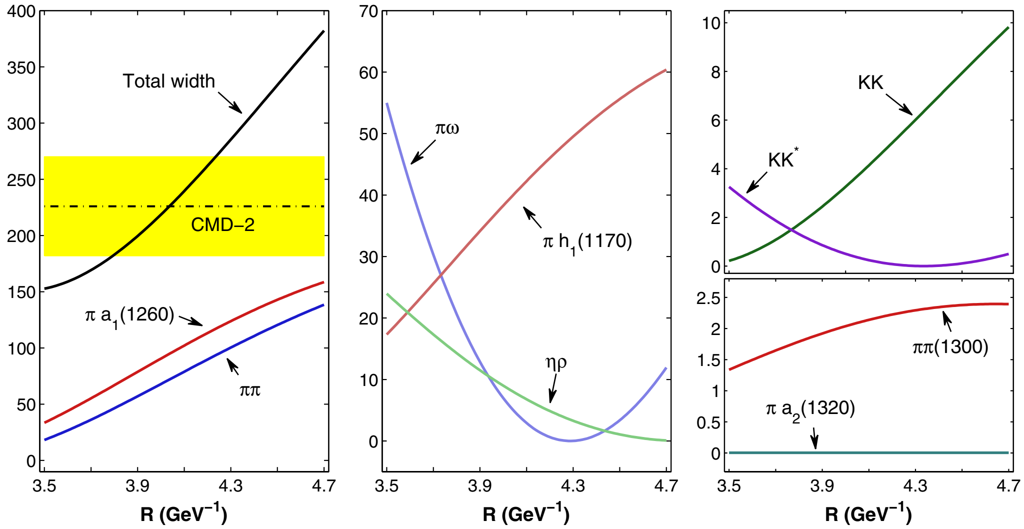

FIG. 2 (color online). The calculated partial and total decay widths of $\rho(1450)$ dependent on the R value. Here, the dashed line with band is the experimental total width from Ref. [101].

corresponding partial decay widths. In the next section, we will compare our theoretical results with the experimental data to perform a phenomenological analysis, which will be helpful to further reveal the underlying properties of these ρ/ρ_3 states.

IV. PHENOMENOLOGICAL ANALYSIS

A. n^3S_1 states

Assuming $\rho(1450)$ as a 2^3S_1 isovector meson, its two-body strong decay behavior is calculated and shown in Fig. 2. Our calculation shows that $\pi\pi$, $\pi a_1(1260)$, $\pi\omega$ and $\pi h_1(1170)$ are its dominant decay modes, where $\pi a_1(1260)$, $\pi\omega$ and $\pi h_1(1170)$ can contribute to the 4π final state. In addition, the obtained width of $\rho(1450) \to \eta\rho$ is also in good agreement with the data in Refs. [1,23]. The partial decay widths of $\rho(1450)$ into $K\bar{K}$, $K\bar{K}^*$ + H.c. and $\pi\pi(1300)$ are small in our calculation. As for $\rho(1450) \to \pi a_2(1320)$, the decay width is tiny. Thus, the experimental data listed in PDG [1] can be quantitatively compared with our results. Given the information of partial decay widths, we obtain the total width of $\rho(1450)$ by summing over all partial decay widths. In Fig. 2, we show the comparison of our results with the CMD-2 data [101], which indicates that there exists a common range between our theoretical total width and the experimental data. Additionally, the obtained total width is also consistent with the experimental width given in Ref. [15], and overlaps with the measured full width listed in Refs. [23,102], which is about 310 MeV.

TABLE III. The obtained ratios of the partial decay widths of the ρ states discussed in Figs. 2–5. Here, we have only listed the ratios weakly dependent on R, which is the reason why we have not listed the ratios of $\Gamma_{\eta\rho}/\Gamma_{\omega\pi}$ and $\Gamma_{KK}/\Gamma_{\omega\pi}$ for $\rho(1450)$ that are strongly dependent on R.

	$\Gamma_{\pi\pi}/\Gamma_{\pi a_1(1260)}$	$\Gamma_{\pi h_1(1170)}/\Gamma_{\pi a_1(1260)}$	$\Gamma_{\pi a_1(1260)}/\Gamma_{\rm Total}$
$\rho(1450)$	0.545–0.873	0.517–0.381	0.219–0.415
$\rho(1700)$	0.400–0.178	0.728–0.696	0.327–0.337
$\rho(1900)$	0.738–1.432	0.470–0.360	0.129–0.262
$\rho(2150)$	2.626–1.674	1.121–0.404	0.009–0.199

Besides providing the information of the partial decay widths of $\rho(1450)$, in Table III several ratios, $\Gamma_{\pi\pi}/\Gamma_{\pi a_1(1260)}$, $\Gamma_{\pi h_1(1170)}/\Gamma_{\pi a_1(1260)}$, and $\Gamma_{\pi a_1(1260)}/\Gamma_{\rm Total}$, are also given, which are weakly dependent on the parameter R. Experimental measurement of these ratios will be a good test of the 2^3S_1 assignment to $\rho(1450)$.

Because of the above analysis, we conclude that it is easy to explain $\rho(1450)$ as a 2^3S_1 state, which is also supported by a recent work in Ref. [103] that claims there is no clear evidence for a hybrid state with $J^{PC} = 1^{--}$.

According to the Regge trajectory analysis, $\rho(1900)$ is a good candidate for a 3^3S_1 state. At present, its resonance parameters are not yet determined experimentally; i.e., different experiments give different results as listed in PDG [1]. The calculated two-body strong decays of $\rho(1900)$ are presented in Fig. 3, where the theoretical total width overlaps with the *BABAR*'s data [29]. In addition, the main decay modes of $\rho(1900)$ are $\pi\pi$, $\pi a_1(1260)$, $\pi h_1(1170)$, $\pi\pi(1300)$, and $\pi\omega(1420)$. Thus, $\rho(1900)$ has a large 4π branching ratio and the decays into $\rho\rho$, $K\bar{K}$, and $\eta b_1(1235)$ are sizeable. In Table III, we also show several ratios of its partial decay widths. These predicted decay behaviors will be helpful to experimentally study $\rho(1900)$ in the future.

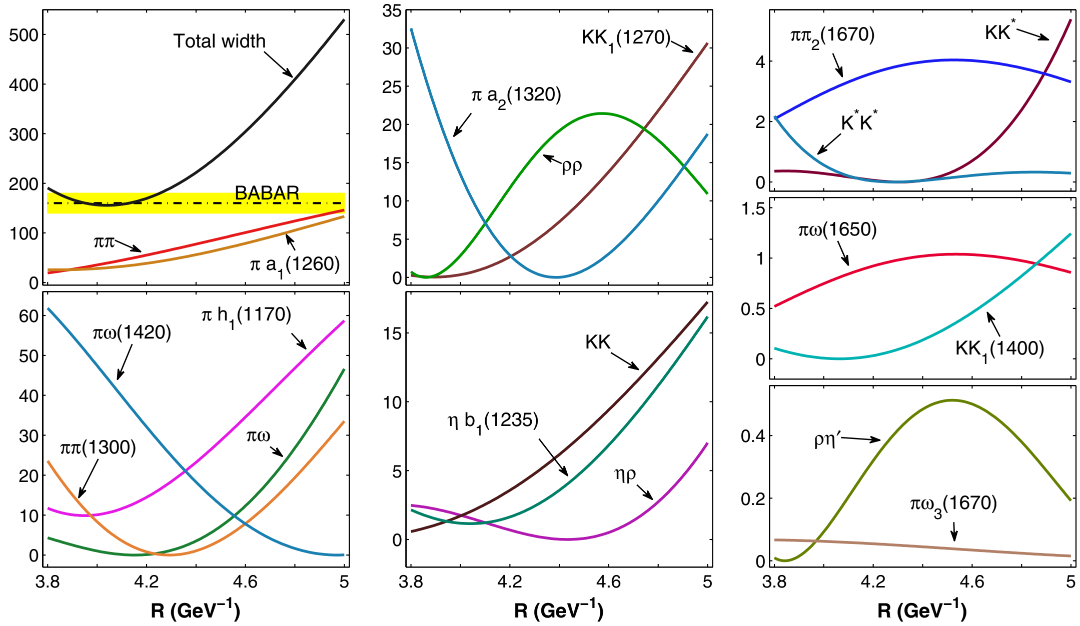

FIG. 3 (color online). The calculated partial and total decay widths of $\rho(1900)$ dependent on the R value. Here, we do not list the decay width of $\rho(1900) \to \pi a_0(1450)$ since this channel is tiny. The dashed line with band is the experimental total width from *BABAR* [29].

As shown in Fig. 1, $\rho(2150)$ can be a 4^3S_1 state. The OZI-allowed two-body strong decay widths are listed in Fig. 4. The obtained total width is dependent on the R value due to the node effect, where the total width is (108–287) MeV corresponding to $R = (4.3\text{–}5.0)\ \mathrm{GeV}^{-1}$. From PDG [1], we notice that the measured total width of $\rho(2150)$ from the e^+e^- interaction is larger than that from the $p\bar{p} \to \pi\pi$ process and S-channel $N\bar{N}$ interaction.

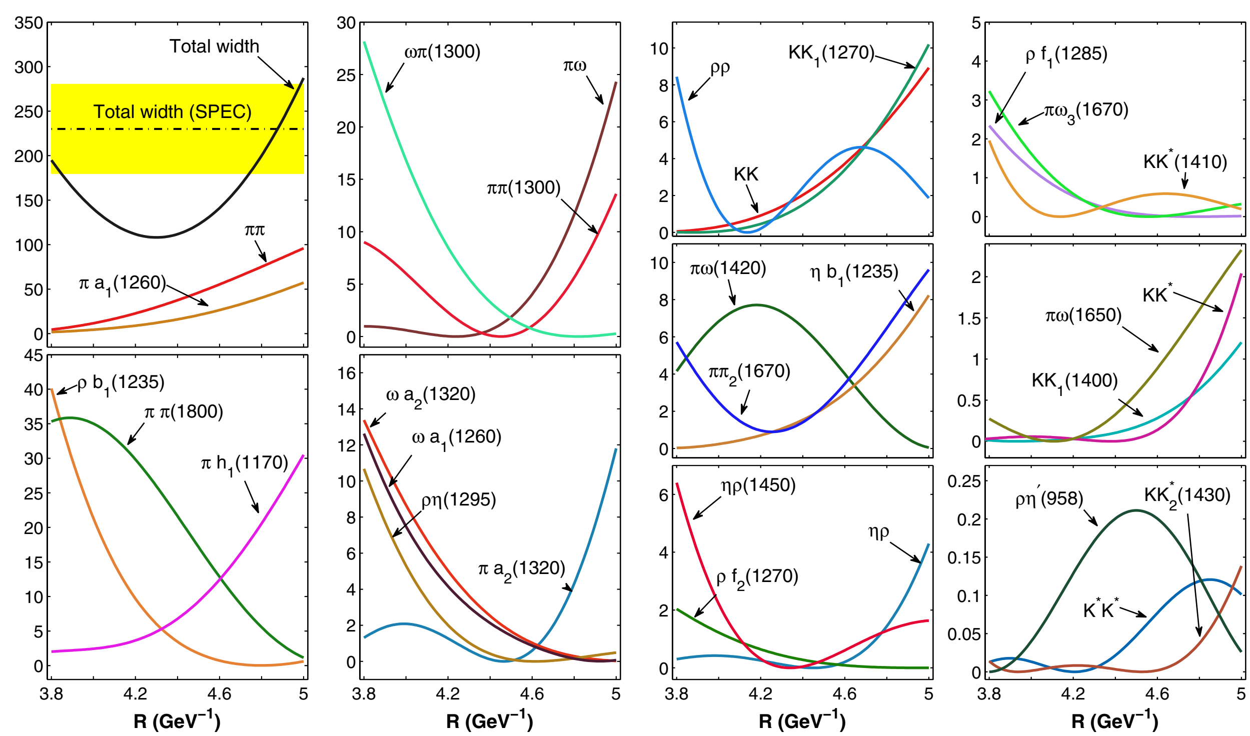

FIG. 4 (color online). The calculated partial and total decay widths of $\rho(2150)$ dependent on the R value. The dashed line with band is the experimental total width taken from Ref. [3].

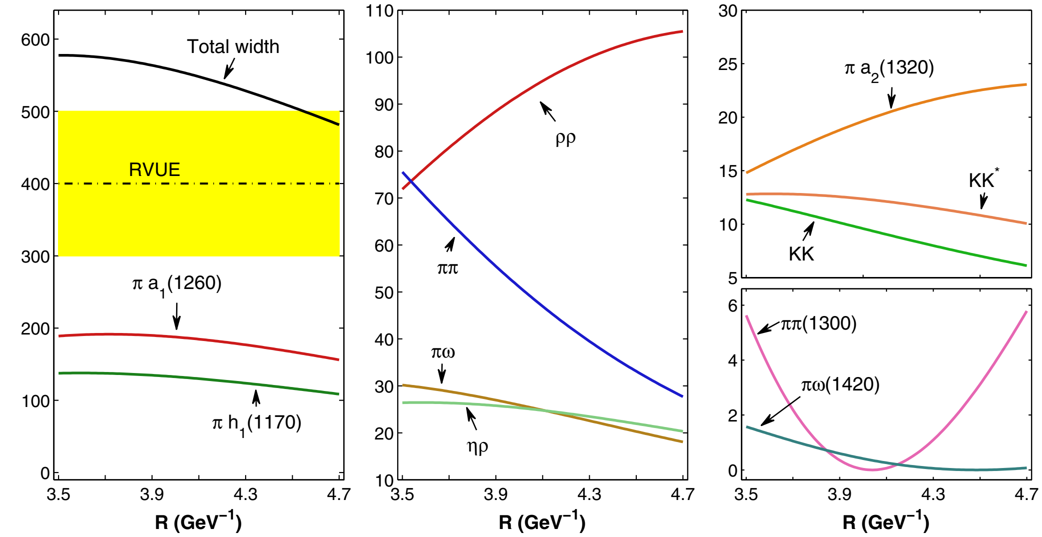

FIG. 5 (color online). The partial and total decay widths of $\rho(1700)$ dependent on the R value. Here, we do not list $\rho(1700) \to \pi a_0(1450)$ due to its tiny decay width. The dashed line with band is the experimental total width from Ref. [23].

Here, the experimental total widths of $\rho(2150)$ are (350 [54], 389 [49], 410 [48], 310 [54]) MeV, (296 [7], 40 [104], 250 [69], 200 [68]) MeV, and (230 [3], 135 [64], 98 [105], 85 [63]) MeV corresponding to the e^+e^- interaction, $p\bar{p} \to \pi\pi$ channel, and S-channel $N\bar{N}$ process, respectively. Our calculation favors the data measured at the $p\bar{p} \to \pi\pi$ process and S-channel $N\bar{N}$ interaction. For example, in Fig. 4 we compare our result of the total width with that in Ref. [3] obtained by analyzing the SPEC's data, where the theoretical and experimental results overlap with each other when $R = (4.74\text{–}4.98)\ \mathrm{GeV}^{-1}$. The calculation of the partial decay widths shows that $\rho(2150)$ decays dominantly into $\pi\pi$, $\pi a_1(1260)$, $\pi\omega$ and $\pi h_1(1170)$. More information on other partial decay widths can be found in Fig. 4. We notice that $\rho(2150)$ was observed in the decay channels $\pi^+\pi^-$, $\omega\pi^0$, $\eta'\pi\pi$,

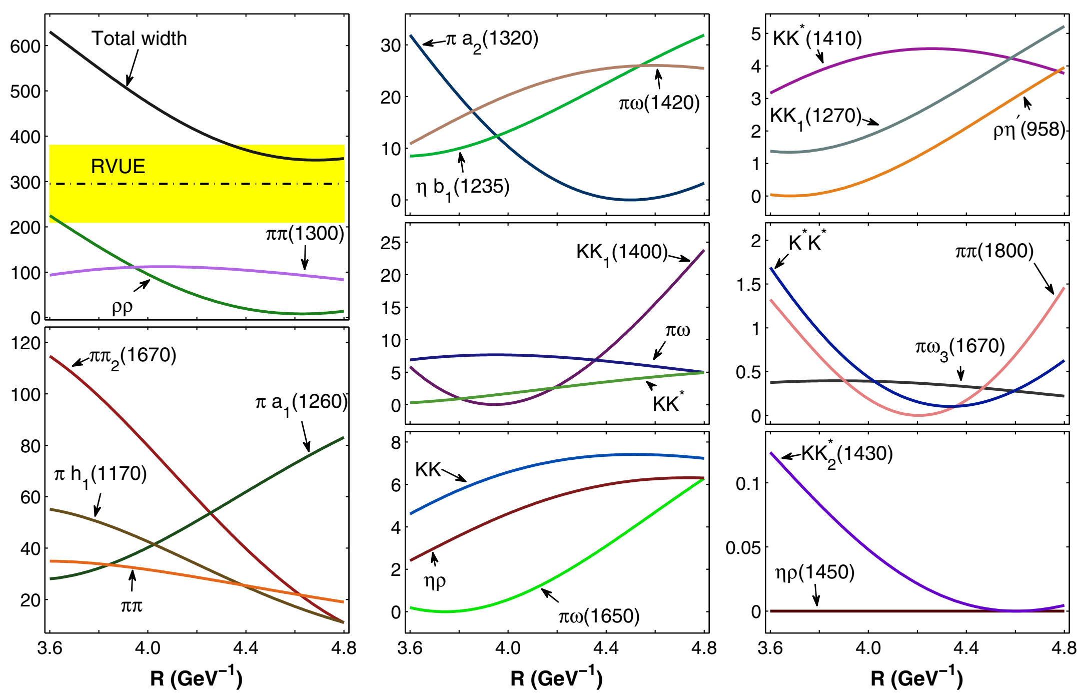

FIG. 6 (color online). The partial and total decay widths of $\rho(2000)$ as the 2^3D_1 state dependent on the R value. The dashed line with band is the experimental total width [4].

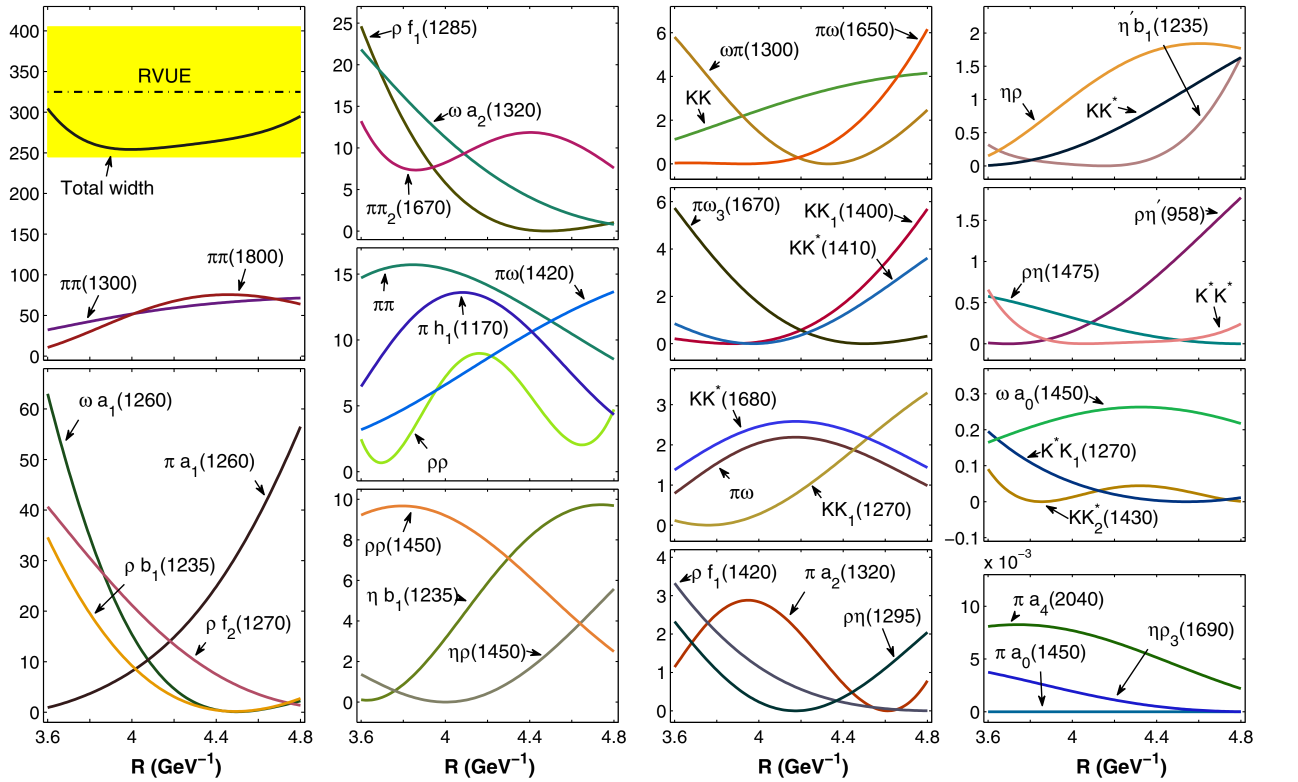

FIG. 7 (color online). The partial and total decay widths of $\rho(2270)$ dependent on the R value. The dashed line with band is the experimental total width [3].

$f_1(1285)\pi\pi$, $\omega\pi\eta$, K^+K^- and 6π [1], which can be reasonably explained by our study. Furthermore, based on the obtained partial decay widths, we also give several ratios of some partial decay widths in Table III, which are also important to test whether $\rho(2150)$ is a 4^3S_1 state.

The ranges of R in Figs. 2–4 needed to reproduce the experimental total widths are (3.79–4.23) GeV^{-1}, (3.85–4.28) GeV^{-1}, and (4.74–4.98) GeV^{-1}, respectively, where the experimental error is considered. These obtained ranges of R also roughly reflect a regularity, i.e., the corresponding R value becomes larger when the radial quantum number increases, which is consistent with the estimate of the potential model [88].

B. n^3D_1 states

The Regge trajectory analysis shows that $\rho(1700)$, $\rho(2000)$, and $\rho(2270)$ can be categorized into the n^3D_1 ρ meson family (see Fig. 1). In this subsection, we discuss their two-body decay behaviors.

As the ground state of the $^3D_1$ ρ meson family, $\rho(1700)$ mainly decays into $\pi a_1(1260)$ and $\pi h_1(1170)$. Of course, $\pi\pi$ and $\rho\rho$ are the important decay channels. These results are consistent with the experimental data [1,23], which naturally explains why $\rho(1700)$ can be found in its 4π and $\rho\pi\pi$ channels. However, the obtained total decay width is larger than most of experimental data listed in PDG. In Fig. 5, we give the comparison between our result and the experimental total width from Ref. [23], where the theoretical total width can overlap the experimental result with error when $R > 4.55$ GeV^{-1}.

In addition, we find that the decay width of $\rho(1700) \to \omega\pi$ is always smaller than that of $\rho(1700) \to \pi\pi$, which does not depend on the R value. This conclusion is consistent with the results in Refs. [23,28,106]. The obtained decay width of $\rho(1700) \to \pi\pi$ is comparable with the value (39 ± 4) MeV given in Ref. [107]. In the Godfrey-Isgur potential model [28], the estimated decay width for $\rho(1700) \to \omega\pi$ is about 25 MeV, which well agrees with our calculation of $\rho(1700) \to \omega\pi$. For the $\rho(1700) \to \eta\rho$ decay, the calculated result is comparable with that listed in Ref. [23]. In Table III, some ratios of the partial decay widths of $\rho(1700)$ are presented.

According to PDG, as for $\rho(1700)$ the ratio $\Gamma_{\pi\pi(1300)}/\Gamma_{4\pi}$ is 0.3, while the ratio $\Gamma_{\pi a_1(1260)}/\Gamma_{4\pi}$ is 0.16

TABLE IV. Several calculated branching ratios of the partial decay widths of $\rho(2000)$ and $\rho(2270)$.

	$\Gamma_{\pi a_1(1260)}/\Gamma_{\pi\pi(1300)}$	$\Gamma_{\pi h_1(1170)}/\Gamma_{\pi\pi}$	$\Gamma_{\pi\pi(1300)}/\Gamma_{\mathrm{Total}}$
$\rho(2000)$	0.300–0.997	0.634–1.714	0.148–0.238
$\rho(2270)$	0.028–0.790	0.439–0.507	0.108–0.253

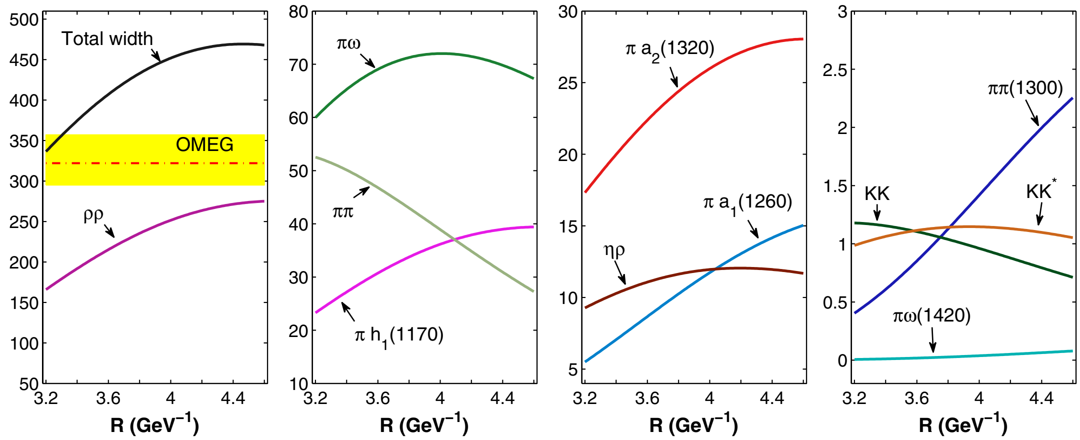

FIG. 8 (color online). The partial and total decay widths of $\rho_3(1690)$ dependent of the R value. The dashed line with band is the experimental total width [108].

(with a large uncertainty) [32]. We need to emphasize that these ratios, $\Gamma_{\pi\pi(1300)}/\Gamma_{4\pi}$ and $\Gamma_{\pi a_1(1260)}/\Gamma_{4\pi}$, listed in PDG can be changed with different considerations of fitting the experimental data (see Sec. 4.3 in Ref. [32] for more details). If adopting these two experimental ratios, the decay into $\pi\pi(1300)$ should be more likely than into $\pi a_1(1260)$. However, we get an order of magnitude larger decay rate into $\pi a_1(1260)$. This discrepancy should be explained when assigning $\rho(1700)$ as a 1^3D_1 state. Introducing the exotic state explanation to $\rho(1700)$ and studying the corresponding decay behavior are an interesting topic.

As the candidate of a 2^3D_1 state, the two-body decay and total decay widths of $\rho(2000)$ are obtained in Fig. 6. The total width can overlap with the Crystal Barrel result in Ref. [4] when $R = (4.34–4.80)\ \text{GeV}^{-1}$. $\rho(2000)$ dominantly decays into $\pi\pi(1300)$, $\rho\rho$, $\pi\pi_2(1670)$ and $\pi a_1(1260)$. The decay channels of the $\rho(2000)$ into $\pi\pi$, $\pi h_1(1170)$, $\pi a_2(1320)$, $\pi\omega(1420)$, and $\eta b_1(1235)$ are also important.

Figure 7 shows the decay information of $\rho(2270)$ from the calculation of the QPC model. Although more decay channels are open, $\rho(2270)$ has a smaller total decay width compared with the former two $^3D_1$ states. The obtained total decay width can overlap with the Crystal Barrel data [3] as shown in Fig. 7. The main decay modes are $\pi\pi(1300)$ and $\pi\pi(1800)$. Other important decay channels include $\pi a_1(1260)$, $\omega a_1(1260)$, $\rho f_2(1270)$, and $\rho b_1(1235)$.

At present, experiments scarcely provide information on $\rho(2270)$. Thus, the theoretical predictions of the two-body strong decays of $\rho(2270)$ shown in Fig. 7 and Table IV can provide valuable guidance to future experimental study on $\rho(2270)$.

In Figs. 5–7, we also notice that the corresponding R values for reproducing the experimental data are within the allowed range.

C. n^3D_3 states

If $\rho_3(1690)$ is a 1^3D_3 state, the partial decay widths are shown in Fig. 8, where the decay of $\rho_3(1690)$ is dominated by the $\rho\rho$ channel. The other large decay modes include $\pi\omega$, $\pi\pi$, and $\pi h_1(1170)$. The decay modes of $\pi a_2(1320)$, $\pi a_1(1260)$, and $\eta\rho$ are also sizeable.

In Table V, several branching ratios of $\rho_3(1690)$ and the ratio $\Gamma_{\pi a_2(1320)}/\Gamma_{\eta\rho}$ are calculated in comparison with the corresponding experimental values. Our branching ratios of $\rho_3(1690) \to \pi\pi$, $\pi\omega$ and the ratio $\Gamma_{\pi a_2(1320)}/\Gamma_{\eta\rho}$ are comparable with the experimental results. At present, experiments reveal that $\rho_3(1690)$ dominantly decays into 4π with the branching ratio $\sim$71.1% [1], which is supported by our calculation, where the final states $\pi\omega$ and $\rho\rho$ can mainly contribute to the 4π final state.

In Fig. 8, we give comparison of our results with the experimental data [108]. If reproducing the experimental total width, the adopted R value is about $3\ \text{GeV}^{-1}$, which is unreasonable. In addition, the obtained total decay width of $\rho_3(1690)$ is larger than the data in PDG [1] when taking R around $4\ \text{GeV}^{-1}$ [88]. This situation shows that $\rho_3(1690)$ as a 1^3D_3 state seems questionable. For clarifying this point, we suggest the precise measurement of its resonance parameters in future experiments. Of course, this discrepancy mentioned above also

TABLE V. Several calculated branching ratios of $\rho_3(1690)$ and the ratio $\Gamma_{\pi a_2(1320)}/\Gamma_{\eta\rho}$. Here, we also list the corresponding experimental data in the third column.

Ratios	This work	Experimental data
$\Gamma_{\rho\rho}/\Gamma_{\text{Total}}$	(49.33–58.79)%	...
$\Gamma_{\pi\pi}/\Gamma_{\text{Total}}$	(5.83–15.62)%	(23.6 ± 1.3)% [1]
$\Gamma_{\pi\omega}/\Gamma_{\text{Total}}$	(14.38–17.83)%	(16 ± 6)% [1]
$\Gamma_{\pi h_1(1170)}/\Gamma_{\text{Total}}$	(6.92–8.42)%	...
$\Gamma_{\pi a_2(1320)}/\Gamma_{\eta\rho}$	1.87–2.40	5.5 ± 2.0 [61]

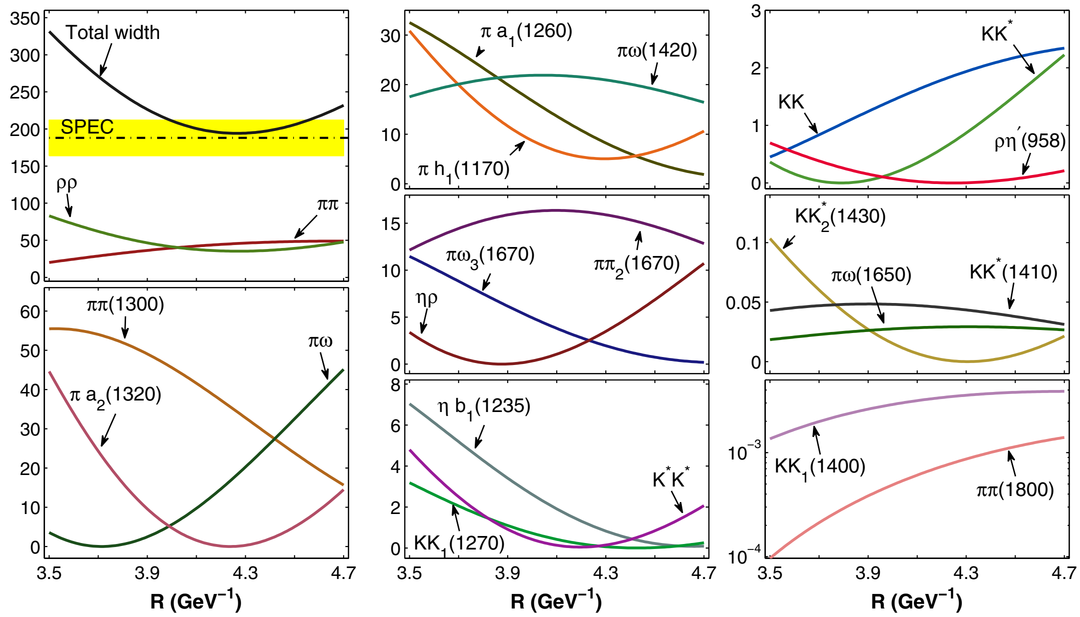

FIG. 9 (color online). The partial and total decay widths of $\rho_3(1990)$ dependent on the R value. Here, the $\pi a_0(1450)$ channel is not listed. The dashed line with band is the experimental total width [3].

provides a possibility of introducing the exotic state explanation to $\rho_3(1690)$. We notice that a three-ρ meson molecular state was proposed in Ref. [62].

The partial decay widths of $\rho_3(1990)$ are predicted in Fig. 9, where the mass of $\rho_3(1990)$ in Table I is adopted in our calculation. $\rho_3(1990)$ mainly decays into $\rho\rho$, $\pi\pi$, $\pi\omega$, $\pi\pi(1300)$, and $\pi\omega$. Several typical decay branching ratios of $\rho_3(1990)$ are presented in Table VI. The calculated total decay width of $\rho_3(1990)$ is compatible with the experimental data [3] as shown in Fig. 9. In addition,

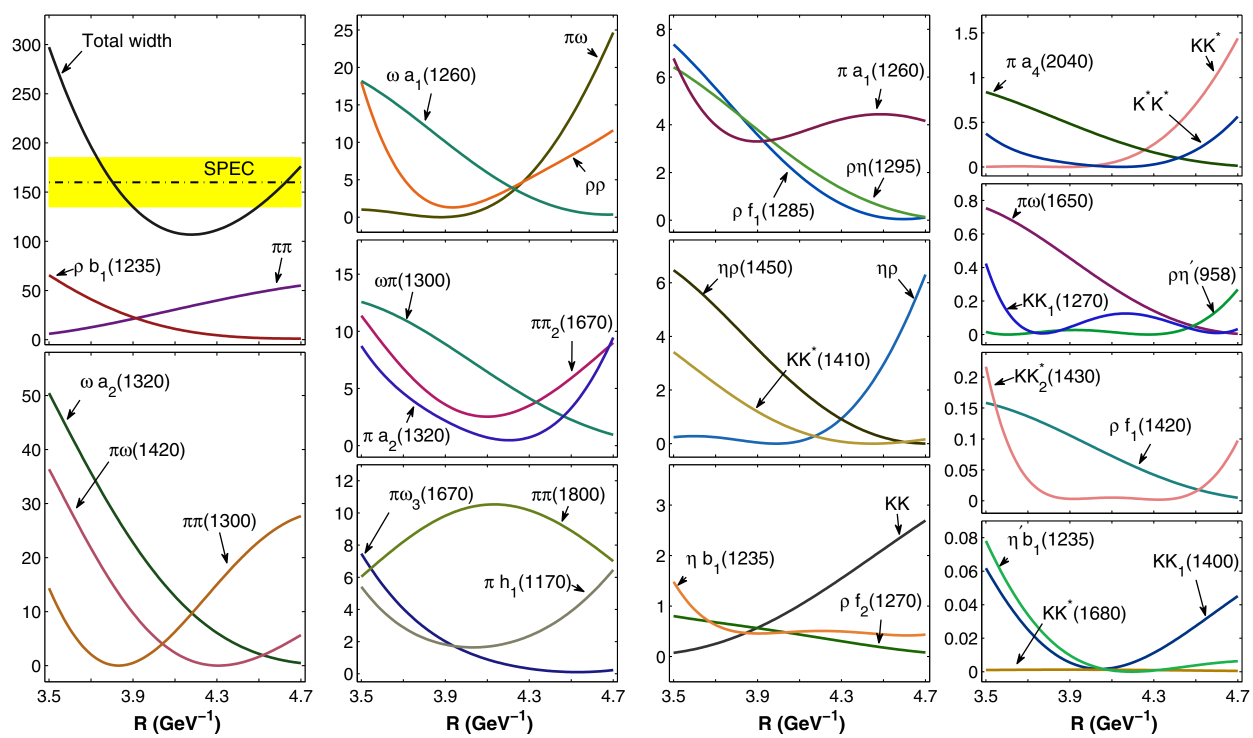

FIG. 10 (color online). The partial and total decay widths of $\rho_3(2250)$ dependent on the R value. Since the decay widths of the $\pi a_0(1450)$, $\rho\rho(1450)$, $K^* K_1(1270)$, and $\rho\eta(1475)$ channels are much smaller than that of the $K\bar{K}^*(1680)$ channel, we do not list these channels here. The dashed line with band is the experimental data [3].

TABLE VI. Some typical branching ratios of $\rho_3(1690)$, $\rho_3(1990)$, and $\rho_3(2250)$.

	$\Gamma_{\rho\rho}/\Gamma_{\text{Total}}$	$\Gamma_{\pi\pi}/\Gamma_{\text{Total}}$	$\Gamma_{\pi\pi(1300)}/\Gamma_{\text{Total}}$
$\rho_3(1690)$	0.493–0.588	0.156–0.058	0.001–0.005
$\rho_3(1990)$	0.250–0.182	0.061–0.240	0.217–0.068
$\rho_3(2250)$	0.010–0.068	0.020–0.358	0.000001–0.168

$\rho_3(1990) \to \pi\pi$, $\pi\omega$ were observed in the experiment [1]. Our calculation shows that the decay widths of $\rho_3(1990) \to \pi\pi$, $\pi\omega$ are sizeable.

In Fig. 10 and Table VI, the decay properties of $\rho_3(2250)$ as a 3^3D_3 are illustrated. For higher ρ_3 meson, the decay behavior reflects the node effect, where $\rho_3(2250)$ decay widths are dependent on the R value. If taking a typical value of $R = 4.62\ \text{GeV}^{-1}$, we can obtain the total decay width consistent with the experimental data [3]. The corresponding main partial decay channels are $\pi\pi$, $\pi\pi(1300)$, and $\pi\omega$. Contrary to the former $\rho_3(1690)$ and $\rho_3(1900)$, the decay width of $\rho_3(2250) \to \rho\rho$ is small. At present, $\rho_3(2250)$ was observed in its $\pi\pi$, $K\bar{K}$, $\eta\pi\pi$, $\pi\omega$, and $\omega a_2(1320)$ decay channels.

V. SUMMARY

In the past decades, many more ρ/ρ_3 states have been observed in experiments. How to categorize these ρ/ρ_3 states into the meson family is an intriguing research topic, which can improve our knowledge of light hadron spectrum. In this work, we systematically study the OZI-allowed two-body strong decay behaviors of the observed ρ/ρ_3 states, where the QPC model [71] is applied to the concrete calculation.

As shown in Fig. 1, the mass spectrum analysis can provide preliminary information on these ρ/ρ_3 states, where their quantum numbers are assigned. Given these assignments, we perform the calculation of two-body strong decays of these ρ/ρ_3 states listed in Table I. By comparing our theoretical results with the existing experimental data, the hadron structure properties of these ρ/ρ_3 states can be obtained and examined.

Besides getting the hadron structure properties of these ρ/ρ_3 states, our study also provides abundant decay information on these states, which can be a valuable guide for further experimental study on the light hadron spectrum.

ACKNOWLEDGMENTS

We would like to thank Qiang Zhao for useful discussions. X. L. also would like to thank Takayuki Matsuki for reading our manuscript carefully. This project is supported by the National Natural Science Foundation of China under Grants No. 11222547, No. 11175073, and No. 11035006, the Ministry of Education of China (FANEDD under Grant No. 200924, SRFDP under Grant No. 20120211110002, NCET, the Fundamental Research Funds for the Central Universities), and the Fok Ying-Tong Education Foundation (No. 131006).

[1] J. Beringer *et al.* (Particle Data Group Collaboration) Phys. Rev. D **86**, 010001 (2012).

[2] B. Aubert *et al.* (*BABAR* Collaboration) Phys. Rev. D **77**, 092002 (2008).

[3] A. V. Anisovich, C. A. Baker, C. J. Batty, D. V. Bugg, L. Montanet, V. A. Nikonov, A. V. Sarantsev, V. V. Sarantsev, and B. S. Zou, Phys. Lett. B **542**, 8 (2002).

[4] A. V. Anisovich, C. A. Baker, C. J. Batty, D. V. Bugg, C. Hodd, H. C. Lu, V. A. Nikonov, A. V. Sarantsev, V. V. Sarantsev, and B. S. Zou, Phys. Lett. B **491**, 47 (2000).

[5] A. V. Anisovich, C. A. Baker, C. J. Batty, D. V. Bugg, V. A. Nikonov, A. V. Sarantsev, V. V. Sarantsev, and B. S. Zou, Phys. Lett. B **508**, 6 (2001).

[6] A. V. Anisovich, C. A. Baker, C. J. Batty, D. V. Bugg, V. A. Nikonov, A. V. Sarantsev, V. V. Sarantsev, and B. S. Zou, Phys. Lett. B **513**, 281 (2001).

[7] A. Hasan and D. V. Bugg, Phys. Lett. B **334**, 215 (1994).

[8] M. A. Abolins, R. L. Lander, W. A. W. Mehlhop, N. huu Xuong, and P. M. Yager, Phys. Rev. Lett. **11**, 381 (1963).

[9] G. P. Yost *et al.* (Particle Data Group Collaboration), Phys. Lett. B **204**, 1 (1988).

[10] G. Cosme, B. Dudelzak, B. Grelaud, B. Jean-Marie, S. Jullian, D. Lalanne, F. Laplanche, V. Lepeltier *et al.*, Nucl. Phys. **B152**, 215 (1979).

[11] C. Bacci, G. De Zorzi, G. Penso, B. Stella, R. Baldini Celio, G. Battistoni, G. Capon, R. Del Fabbro *et al.*, Nucl. Phys. **B184**, 31 (1981).

[12] L. M. Barkov, A. G. Chilingarov, S. I. Eidelman, B. I. Khazin, M. Y. Lelchuk, V. S. Okhapkin, E. V. Pakhtusova, S. I. Redin *et al.*, Nucl. Phys. **B256**, 365 (1985).

[13] S. I. Dolinsky, V. P. Druzhinin, M. S. Dubrovin, S. I. Eidelman, V. B. Golubev, V. N. Ivanchenko, I. A. Koop, A. A. Mikhailichenko *et al.*, Phys. Lett. B **174**, 453 (1986).

[14] C. Erkal and M. G. Olsson, Z. Phys. C **31**, 615 (1986).

[15] A. Donnachie and H. Mirzaie, Z. Phys. C **33**, 407 (1987).

[16] A. Donnachie and A. B. Clegg, Z. Phys. C **34**, 257 (1987).

[17] A. B. Clegg and A. Donnachie, Z. Phys. C **40**, 313 (1988).

[18] S. Fukui, N. Horikawa, S. Inaba, T. Inagaki, Y. Inagaki, Y. Ishizaki, T. Iwata, T. Kinashi *et al.*, Phys. Lett. B **202**, 441 (1988).

[19] A. Antonelli *et al.* (DM2 Collaboration), Phys. Lett. B **212**, 133 (1988).

[20] D. Bisello *et al.* (DM2 Collaboration), Phys. Lett. B **220**, 321 (1989).

[21] A. Castro *et al.* (DM2 Collaboration), Report No. LAL-88-58.

[22] S. I. Dolinsky, V. P. Druzhinin, M. S. Dubrovin, V. B. Golubev, V. N. Ivanchenko, E. V. Pakhtusova, A. N. Peryshkin, S. I. Serednyakov *et al.*, Phys. Rep. **202**, 99 (1991).
[23] A. B. Clegg and A. Donnachie, Z. Phys. C **62**, 455 (1994).
[24] A. Donnachie and A. B. Clegg, Phys. Rev. D **51**, 4979 (1995).
[25] N. N. Achasov and A. A. Kozhevnikov, Phys. Rev. D **55**, 2663 (1997).
[26] N. N. Achasov and A. A. Kozhevnikov, Phys. Rev. D **62**, 117503 (2000).
[27] M. N. Achasov, V. M. Aulchenko, A. Y. Barnyakov, K. I. Beloborodov, A. V. Berdyugin, A. G. Bogdanchikov, A. A. Botov, T. V. Dimova *et al.*, arXiv:1303.5198.
[28] S. Godfrey and N. Isgur, Phys. Rev. D **32**, 189 (1985).
[29] T. Barnes, F. E. Close, P. R. Page, and E. S. Swanson, Phys. Rev. D **55**, 4157 (1997).
[30] A. B. Arbuzov, E. A. Kuraev, and M. K. Volkov, Phys. At. Nucl. **74**, 726 (2011).
[31] M. K. Volkov, D. Ebert, and M. Nagy, Int. J. Mod. Phys. A **13**, 5443 (1998).
[32] A. Abele *et al.* (CRYSTAL BARREL Collaboration), Eur. Phys. J. C **21**, 261 (2001).
[33] F. E. Close and P. R. Page, Nucl. Phys. **B443**, 233 (1995).
[34] A. Donnachie and Y. S. Kalashnikova, Z. Phys. C **59**, 621 (1993).
[35] F. E. Close and P. R. Page, Phys. Rev. D **56**, 1584 (1997).
[36] A. Donnachie and Y. S. Kalashnikova, Phys. Rev. D **60**, 114011 (1999).
[37] L. Y. Glozman, C. B. Lang, and M. Limmer, Phys. Lett. B **705**, 129 (2011).
[38] L. Y. Glozman, AIP Conf. Proc. **1354**, 64 (2011).
[39] D. V. Bugg, Phys. Rev. D **87**, 118501 (2013).
[40] K. Kittimanapun, K. Khosonthongkee, C. Kobdaj, P. Suebka, and Y. Yan, Phys. Rev. C **79**, 025201 (2009).
[41] A. Antonelli *et al.* (FENICE Collaboration), Phys. Lett. B **365**, 427 (1996).
[42] P. L. Frabetti *et al.* (E687 Collaboration), Phys. Lett. B **514**, 240 (2001).
[43] P. L. Frabetti, H. W. K. Cheung, J. P. Cumalat, C. Dallapiccola, J. F. Ginkel, W. E. Johns, M. S. Nehring, E. W. Vaandering *et al.*, Phys. Lett. B **578**, 290 (2004).
[44] B. Aubert *et al.* (*BABAR* Collaboration), Phys. Rev. D **73**, 052003 (2006).
[45] E. P. Solodov (CMD3 Collaboration), arXiv:1108.6174.
[46] D. Bisello, J. C. Bizot, J. Buon, A. Cordier, B. Delcourt, and F. Mane, Phys. Lett. **107B**, 145 (1981).
[47] M. Atkinson *et al.* (Omega Photon Collaboration), Z. Phys. C **29**, 333 (1985).
[48] A. B. Clegg and A. Donnachie, Z. Phys. C **45**, 677 (1990).
[49] M. E. Biagini, S. Dubnicka, E. Etim, and P. Kolar, Nuovo Cim. A **104**, 363 (1991).
[50] S. Dubnicka, Nuovo Cim. A **100**, 1 (1988).
[51] D. Alde *et al.* (IHEP-IISN-LANL-LAPP-KEK Collaboration), Z. Phys. C **54**, 553 (1992).
[52] D. Alde *et al.* (GAMS Collaboration), Nuovo Cim. A **107**, 1867 (1994); Z. Phys. C **66**, 379 (1995).
[53] A. V. Anisovich, V. A. Nikonov, A. V. Sarantsev, V. V. Sarantsev, C. A. Baker, C. J. Batty, D. V. Bugg, A. Hasan *et al.*, Phys. Lett. B **471**, 271 (1999).
[54] B. Aubert *et al.* (*BABAR* Collaboration), Phys. Rev. D **76**, 092005 (2007); **77**, 119902 (2008).
[55] A. V. Anisovich, V. V. Anisovich, and A. V. Sarantsev, Phys. Rev. D **62**, 051502 (2000).
[56] P. Masjuan, E. R. Arriola, and W. Broniowski, Phys. Rev. D **85**, 094006 (2012).
[57] P. Masjuan, E. R. Arriola, and W. Broniowski, Phys. Rev. D **87**, 118502 (2013).
[58] D. V. Bugg, Phys. Rep. **397**, 257 (2004).
[59] M. Goldberg, Phys. Lett. **17**, 354 (1965).
[60] A. Forino and R. Gessaroli, Phys. Lett. **19**, 65 (1965).
[61] D. V. Amelin *et al.* (VES Collaboration), Nucl. Phys. **A668**, 83 (2000).
[62] L. Roca and E. Oset, Phys. Rev. D **82**, 054013 (2010).
[63] R. J. Abrams, R. L. Cool, G. Giacomelli, T. F. Kycia, B. A. Leontic, K. K. Li, and D. N. Michael, Phys. Rev. D **1**, 1917 (1970).
[64] M. Coupland, E. Eisenhandler, W. R. Gibson, P. I. P. Kalmus, and A. Astbury, Phys. Lett. **71B**, 460 (1977).
[65] D. Cutts, M. Good, P. Grannis, D. Green, Y. Lee, R. Pittman, J. Storer, A. Benvenuti, G. Fischer, and D. Reeder, Phys. Rev. D **17**, 16 (1978).
[66] A. A. Carter, Nucl. Phys. **B141**, 467 (1978).
[67] A. A. Carter, M. Coupland, E. Eisenhandler, W. R. Gibson, P. I. P. Kalmus, D. P. Kimber, A. Astbury, and D. P. Jones, Phys. Lett. **67B**, 117 (1977).
[68] A. D. Martin and M. R. Pennington, Nucl. Phys. **B169**, 216 (1980).
[69] B. R. Martin and D. Morgan, Nucl. Phys. **B176**, 355 (1980).
[70] G. F. Chew and S. C. Frautschi, Phys. Rev. Lett. **8**, 41 (1962).
[71] L. Micu, Nucl. Phys. **B10**, 521 (1969).
[72] A. Le Yaouanc, L. Oliver, O. Pene, and J. C. Raynal, Phys. Rev. D **8**, 2223 (1973).
[73] A. Le Yaouanc, L. Oliver, O. Pene, and J.-C. Raynal, Phys. Rev. D **9**, 1415 (1974).
[74] A. Le Yaouanc, L. Oliver, O. Pene, and J. C. Raynal, Phys. Rev. D **11**, 1272 (1975).
[75] A. Le Yaouanc, L. Oliver, O. Pene, and J. C. Raynal, Phys. Lett. **72B**, 57 (1977).
[76] A. Le Yaouanc, L. Oliver, O. Pene, and J.-C. Raynal, Phys. Lett. **71B**, 397 (1977); *Hadron Transitions of the Quark Model* (Gordon and Breach, New York, 1988).
[77] E. van Beveren, C. Dullemond, and G. Rupp, Phys. Rev. D **21**, 772 (1980); **22**, 787 (1980).
[78] E. van Beveren, G. Rupp, T. A. Rijken, and C. Dullemond, Phys. Rev. D **27**, 1527 (1983).
[79] R. Bonnaz, B. Silvestre-Brac, and C. Gignoux, Eur. Phys. J. A **13**, 363 (2002).
[80] W. Roberts and B. Silvestre-Brac, Few-Body Syst. **11**, 171 (1992).
[81] J. Lu, W.-Z. Deng, X.-L. Chen, and S.-L. Zhu, Phys. Rev. D **73**, 054012 (2006).
[82] Z.-G. Luo, X.-L. Chen, and X. Liu, Phys. Rev. D **79**, 074020 (2009).
[83] H. G. Blundell and S. Godfrey, Phys. Rev. D **53**, 3700 (1996).
[84] P. R. Page, Nucl. Phys. **B446**, 189 (1995).
[85] S. Capstick and N. Isgur, Phys. Rev. D **34**, 2809 (1986).
[86] S. Capstick and W. Roberts, Phys. Rev. D **49**, 4570 (1994).
[87] E. S. Ackleh, T. Barnes, and E. S. Swanson, Phys. Rev. D **54**, 6811 (1996).

[88] F. E. Close and E. S. Swanson, Phys. Rev. D **72**, 094004 (2005).
[89] H. Q. Zhou, R. G. Ping, and B. S. Zou, Phys. Lett. B **611**, 123 (2005).
[90] X.-H. Guo, H.-W. Ke, X.-Q. Li, X. Liu, and S.-M. Zhao, Commun. Theor. Phys. **48**, 509 (2007).
[91] B. Zhang, X. Liu, W.-Z. Deng, and S.-L. Zhu, Eur. Phys. J. C **50**, 617 (2007).
[92] C. Chen, X.-L. Chen, X. Liu, W.-Z. Deng, and S.-L. Zhu, Phys. Rev. D **75**, 094017 (2007); X. Liu, C. Chen, W. Z. Deng, and X. L. Chen, Chinese Phys. C **32**, 424 (2008).
[93] D.-M. Li and B. Ma, Phys. Rev. D **77**, 074004 (2008); **77**, 094021 (2008); D.-M. Li and S. Zhou, Phys. Rev. D **78**, 054013 (2008); **79**, 014014 (2009).
[94] Z.-F. Sun and X. Liu, Phys. Rev. D **80**, 074037 (2009).
[95] X. Liu, Z.-G. Luo, and Z.-F. Sun, Phys. Rev. Lett. **104**, 122001 (2010).
[96] Z.-F. Sun, J.-S. Yu, X. Liu, and T. Matsuki, Phys. Rev. D **82**, 111501 (2010).
[97] J.-S. Yu, Z.-F. Sun, X. Liu, and Q. Zhao, Phys. Rev. D **83**, 114007 (2011).
[98] X. Wang, Z.-F. Sun, D.-Y. Chen, X. Liu, and T. Matsuki, Phys. Rev. D **85**, 074024 (2012).
[99] Z.-C. Ye, X. Wang, X. Liu, and Q. Zhao, Phys. Rev. D **86**, 054025 (2012).
[100] M. Jacob and G. C. Wick, Ann. Phys. (N.Y.) **7**, 404 (1959); Ann. Phys. (N.Y.) **281**, 774 (2000).
[101] R. R. Akhmetshin *et al.* (CMD-2 Collaboration), Phys. Lett. B **509**, 217 (2001).
[102] C. Caso *et al.* (Particle Data Group Collaboration), Eur. Phys. J. C **3**, 1 (1998).
[103] B. Ketzer, Proc. Sci., QNP (2012) 025.
[104] M. N. Oakden and M. R. Pennington, Nucl. Phys. **A574**, 731 (1994).
[105] J. Alspector, K. Cohen, W. Harrison, B. Maglich, F. Sannes, D. Van Harlingen, G. Cvijanovich, M. Matin, and J. Oostens, Phys. Rev. Lett. **30**, 511 (1973).
[106] R. Kokoski and N. Isgur, Phys. Rev. D **35**, 907 (1987).
[107] D. V. Bugg, B. S. Zou, and A. V. Sarantsev, Nucl. Phys. **B471**, 59 (1996).
[108] M. J. Corden, J. D. Dowell, J. Garvey, M. Jobes, I. R. Kenyon, J. Mawson, T. McMahon, I. F. Corbett *et al.*, Nucl. Phys. **B157**, 250 (1979).